WIRELESS COMMUNICATIONS AND MOBILE COMPUTING
Wirel. Commun. Mob. Comput. 2015; **15**:260–275
Published online 28 December 2012 in Wiley Online Library (wileyonlinelibrary.com). DOI: 10.1002/wcm.2335

RESEARCH ARTICLE

Multicast communications in cognitive radio networks using directional antennas

Wenxuan Guo[1]* and Xinming Huang[2]

[1] Active Broadband Networks, 20 Speen St., Framingham, MA 01701, U.S.A.
[2] Department of Electrical and Computer Engineering, Worcester Polytechnic Institute, Worcester, MA 01609, U.S.A.

ABSTRACT

This paper presents a study on multicast communications in cognitive radio networks (CRNs)using directional antennas. The objective is to maximize the throughput of the CRN. The spectrum is divided into multiple channels and licensed to the primary network. While the CRN is accessing the spectrum, the interference power is carefully controlled to avoid impacting the operation of the primary network. The mathematical model is presented and subsequently formulated as a mixed integer non-linear programming (MINLP) problem, which is non-deterministic polynomial-time hard. Therefore, a greedy algorithm is designed to approximate the optimal performance. The MINLP problem is then relaxed and an upper bound is developed. Simulation results are presented to compare the performance of the greedy algorithm and the upper bound, which demonstrates the efficacy of the greedy algorithm as well as the tightness of the upper bound. Copyright © 2012 John Wiley & Sons, Ltd.

KEYWORDS
cognitive radio networks; directional antenna; multicast communication

***Correspondence**
Wenxuan Guo, Active Broadband Networks, 20 Speen St., Framingham, MA 01701, U.S.A.
E-mail: wenxuanguo@gmail.com

1. INTRODUCTION

In order to fully utilize the scarce spectrum resources, emerging cognitive radio technology becomes a promising approach to exploit the under-utilized spectrum [1]. In a cognitive radio network (CRN), unlicensed wireless users (secondary users) are allowed to dynamically access the licensed bands, as long as the licensed wireless users (primary users) in those particular bands are not interfered. Wireless devices equipped with cognitive radios are enabled to implement various functionalities, including frequency agility, transmit power control and access coordination, which render more efficient use of available spectrum.

In this paper, we consider a CRN that consists of multiple base stations (BSs) and secondary users (SUs). Each BS supports a set of SUs. The spectrum of interest is divided into a set of multiple orthogonal channels using frequency division multiple access, which are licensed to primary users (PUs). We assume that the channel usage pattern for PUs is quasi-static so that SUs have ample time to implement primary-user detection and thereby avoid interfering with PUs' connections. We consider the scenario of multicast communication in the CRN. An example deployment of a CRN is depicted in Figure 1.

Cognitive radio networks may operate in infrastructure-based systems. As a practical application, IEEE 802.22 based regional area networks dynamically allocate TV spectrum to SUs [2] while they keep provisioning service to PUs. The TV bands are selected because they feature very favorable propagation characteristics and are scarcely used because of popularity of cable and satellite TV services. Therefore, CRN must avoid interfering with PUs in PRN as the licensed TV customers by carefully controlling its beam configuration and channel selection. Because TV signals are transmitted from BSs to users, only downlink scenario is considered in this paper.

Directional antenna in the context of wireless networks can largely reduce the radio interference, thereby improving the utilization of wireless medium and consequently the network performance. In addition, directional antennas permit energy savings by concentrating transmission energy where it is needed. Directional antennas can be loosely classified into omni-directional antennas, modestly directional antennas and highly directional antennas. Omni-directional antennas have fixed beamwidth

Copyright © 2012 John Wiley & Sons, Ltd.

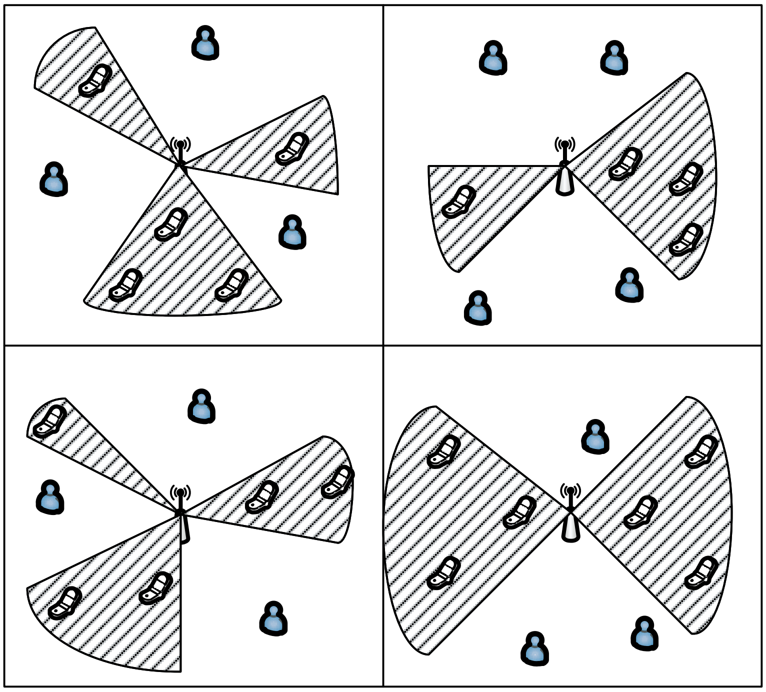

Figure 1. An example deployment of a cognitive radio network. Head portraits represent primary users. Cell phones represent secondary users.

and unsteerable orientation. Modestly directional antennas have fixed beamwidth and steerable orientation. At last, highly directional antennas have variable beamwidth and steerable orientation. In fact, the omni-directional antennas and modestly directional antennas are special cases of the highly directional antennas. In this paper, we are mainly discussing the highly directional antennas.

In this paper, we study the joint problem of antenna directionality and channel assignment (ADCA) to maximize the CRN throughput, which is defined as the sum rate of all links supporting SUs. Because transmitters only interfere with user nodes in their directional coverage area, antenna beamwidth and orientation exert a great role in network throughput performance. Given a configuration of directional antennas, the network throughput can be greatly improved by intelligent channel assignment in terms of spatial diversity. Therefore, ADCA are mutually affected and of great importance to CRN throughput.

To formulate the ADCA problem mathematically, we characterize behaviors and constraints for multiple parameters from a multicast CRN. Special attention is given to modeling of antenna directionality, beam covering, channel assignment and interference modeling. Because the formulation of the ADCA problem falls into mixed integer non-linear programming (MINLP), which is non-deterministic polynomial-time hard (NP-hard) in general, we aim to derive a near-optimal solution. In particular, we propose a greedy algorithm to iteratively increase the overall throughput. During each iteration, one BS is chosen to build multicast links with SUs to produce maximum throughput increase, which can be formulated as a mixed integer linear programming (MILP) problem and solved by the branch and bound algorithm. Because the solution obtained by the proposed greedy algorithm represents a lower bound for the objective, we compare it with the upper bound developed later. Simulations show that the performance obtained by the greedy algorithm are very close to the upper bound, thus suggesting the following: (i) that the upper bound is very tight; and (ii) that the solution obtained by the greedy algorithm is near-optimal.

The rest of this paper is organized as follows. In Section 2, we review the related work about channel assignment and directional antenna. In Section 3, we describe the network model. In Section 4, we propose a greedy algorithm to solve the ADCA problem. In Section 5, simulation results are presented to compare the solutions obtained by the greedy algorithm and the upper bound. Section 8 concludes this paper.

2. RELATED WORK

This paper is related to our previous work [3]. Although sharing the same objective, this paper is mainly concerned with ADCA, while deferring power control as a future work.

Adaptive phased-array antennas and specifically directional antennas are being given significant attention in recent times, especially in the context of *ad hoc* networks. In [4], the authors presented a constraint formulation in terms of MILP, which can be used for an optimal solution of the minimum-energy multicast problem in wireless *ad hoc* networks with directional antennas. In [5], the authors identified several criteria and investigated the impact on overall system performance in the context of *ad hoc* wireless networks with directional antennas, that is reducing radio interference and improving the utilization of wireless medium. In [6], the authors consider a wireless *ad hoc* network where each node employs a single-beam directional antenna and is provisioned with limited energy. An online routing algorithm was proposed for successive multicast communication requests with the aim of maximizing the network lifetime. There are also papers using directional antennas on wireless mesh networks (MWNs). In [7], an analytical model is derived, which allows the incorporation of various node distribution models, radio channel models and antenna models. In [8], DMesh, a WMN architecture was proposed that combines spatial separation from directional antennas with frequency separation from orthogonal channels to improve the throughput of WMNs. In addition, a distributed, directional channel assignment algorithm was proposed for mesh routers that effectively exploits the spatial and frequency separation opportunities in a DMesh network.

The concept of cognitive radio was first coined by Mitola in his dissertation work [9] and later in his visionary paper [10]. Haykin provides a thorough overview of cognitive radio and describes the fundamental cognitive capabilities and cognitive tasks [11]. A cognitive radio is defined as an intelligent wireless communications system that is capable of sensing its surrounding environment, learning from experience, and adapting certain operating parameters (e.g., transmit-power, carrier-frequency, and modulation strategy) in real-time [11]. There are two primary objectives: highly reliable communications whenever and wherever needed and efficient utilization of the radio spectrum. Akyildiz *et al*. give a survey on the dynamic spectrum access for cognitive radios [1,12]. The basic concept of CRN is described by Thomas *et al*. together with a case study to illustrate how such a network might operate [13]. In [14], the concept of cognitive radio is extended to multihop networks.

A number of channel assignment schemes has been proposed in recent years. In [15], a distributed and adaptive approach is proposed to manage spectrum usage in dynamic spectrum access networks. However, this paper does not take into account the control of transmit power. In addition, the more practical physical interference model is not studied. In [16], Chin *et al*. address the problem of dynamically assigning channels in *ad hoc* wireless networks via power control to satisfy their minimum QoS requirements. The objective then is to maximize the number of co-channel links subject to some stability conditions. In [17], a cluster-based multipath topology control and channel assignment scheme is proposed, which explicitly creates a separation between the channel assignment and topology control functions, thus minimizes flow disruptions. In [18], Raniwala *et al*. propose a greedy load-aware channel assignment scheme when network nodes are with multiple radios. The goal of channel assignment is to bind each network interface to a radio channel such that the available bandwidth on each link is proportional to its expected load. In [19], Alicherry *et al*. mathematically formulate the joint channel assignment and routing problem, taking into account the interference constraints, the number of channels in the network and the number of radios available at each mesh router. A centralized algorithm is developed to solve the problem to yield the optimized network throughput. The channel assignment algorithm is used to adjust the flow on the flow graph to keep the increase of interference for each channel to a minimum. In [20], Ramachandran *et al*. propose an interference-aware channel assignment algorithm and protocol for multi-radio WMNs. The proposed solution intelligently assigns channels to radios to minimize interference and thus enhance network performance.

Multicast communication on CRNs has been extensively researched recently. In [21], a cross-layer optimization approach is proposed to multicast video in CRNs. The problem is to optimize the overall received video quality as well as achieving fairness. Important design factors are considered, including video coding, rate control, spectrum sensing and spectrum access. However, the model employed only involves one BS. In [22], an optimization framework for multicast scheduling in CRNs is presented. Eventually, two multicast scheduling algorithms are proposed accordingly. In [23], Ren *et al*. address the multicast problem in CRNs. A low complexity algorithm is proposed to construct the minimum-energy multicast tree and transform the original problem into a directed Steiner tree problem. However, few research works have addressed the multicast problem for CRNs involving multiple BSs and directional antennas.

3. PROBLEM MODELING

We consider a CRN that consists of multiple BSs and SUs. Each BS supports a set of SUs. The spectrum of interest is divided into a set of multiple orthogonal channels using frequency division multiple access, which are licensed to PUs. We assume that the channel usage pattern for PUs remain static so that SUs have time to implement primary-user detection and thereby avoid interfering with PUs' connections. From this observation, the studied CRNs should satisfy both demanding delay-sensitive and loss-sensitive applications. Therefore, both video multicast and data multicast can be applied to our proposed model.

To explore advantages offered by the use of directional antennas, we consider the scenario of downlink multicast traffic in the CRN. Each BS employs exactly one channel to support one or multiple SUs.

Table I lists frequently used notations in this section.

Table I. Notation.

Symbol	Definitions
B	The number of BSs
N	The number of SUs
C	The number of channels
Q	The number of tunable angle beamwidths
λ	A number of very large value
γ	The minimum signal to interference and noise ratio (SINR)
b_i	The ith BS
s_j	The jth SU
p_j	The jth PU
$\theta_{\min}$	The minimum angle of beamwidth
$t_i^{k,q}$	Binary variable indicating if channel k of b_i has beamwidth $q\theta_{\min}$
$x_{i,j}^{k,q}$	Binary variable indicating the assignment of b_i to s_j when $t_i^{k,q}$=1
$y_{i,j}^{k,q}$	Binary variable indicating b_i covers s_j when $t_i^{k,q}$=1
$y_{i,j}^{k,q1}, y_{i,j}^{k,q2}$	Two binary variables decomposed from $y_{i,j}^{k,q}$
φ_i^k	The antenna orientation of b_i on channel k
θ_i^k	The beamwidth of b_i on channel k
$\beta_{i,j}$	The counter-clockwise angle of the line from b_i to s_j
$l_{i,j}^{k,q}$	The link between b_i and s_j when $t_i^{k,q}$=1
$p_{i,j}^{k,q}$	The received power of $l_{i,j}^{k,q}$
$d_{i,j}$	The distance of b_i and s_j
$c_{i,j}^{k,q}$	The rate of $l_{i,j}^{k,q}$
N_0	The ambient noise power
ζ	The interference threshold value to protect PUs
k_{j*}	The channel on which p_j operates
$p_{i,j*}^{k_{j*},q}$	The power received on p_j from b_i when $t_i^{k_{j*},q} = 1$
$y_{i,j*}^{k_{j*},q}$	Binary variable indicating b_i covers p_j when $t_i^{k_{j*},q} = 1$
$y_{i,j*}^{k_{j*},q1}$, $y_{i,j*}^{k_{j*},q2}$	Binary variables decomposed from $y_{i,j*}^{k_{j*},q}$
$\beta_{i,j*}$	The counter-clockwise angle of the line from b_i to p_j

BS, base stations; SU, secondary user; PU, primary user.

3.1. Directional antenna model

We use a directional antenna propagation model as shown in Figure 2, where antenna orientation $\varphi_u (0 \le \varphi_u < 2\pi)$ of node u is defined as the angle measured counter-clockwise from the horizontal axis to the first side of the beam. The antenna beamwidth is specified as the angle of $\theta_u (\theta_{\min} \le \theta_u \le 2\pi)$, where $\theta_{\min}$ denotes the minimum angle of beamwidth. To model the discrete version of antenna beamwidth, we introduce an integer parameter Q that represents the total number of angle values to which the beamwidth can be adjusted, that is, $\theta_{\min}, 2\theta_{\min}, \ldots, Q\theta_{\min}$ ($Q\theta_{\min} \le 2\pi$). We introduce binary variable $t_i^{k,q}$ indicating if the ith BS b_i's beam on channel k has beamwidth $q\theta_{\min}$ when $t_i^{k,q} = 1$. Obviously, it is required that $\sum_{q=1}^{Q} t_i^{k,q} \le 1 \forall i, k$.

Definition: A joint downlink channel assignment, power control and antenna directionality scheme is specified by a matrix $\boldsymbol{X}$, which is defined as (1).

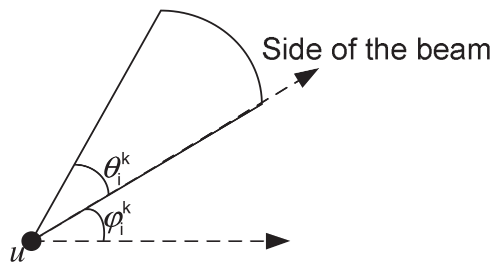

Figure 2. Directional antenna propagation model.

$$\mathbf{X} = \{x_{i,j}^{k,q} | x_{i,j}^{k,q} \in \{0,1\}, i \in \{1,2,...,B\}, j \in \{1,2,...,N\}, k \in \{1,2,...,C\}, q \in \{1,2,...,Q\} \tag{1}$$

$x_{i,j}^{k,q}$ is denoted as the binary variable with $x_{i,j}^{k,q} = 1$ indicating the assignment of the kth channel of b_i to the jth SU s_j when the beamwidth of the transmitter antenna is of $q\theta_{\min}$. Similarly, denote $y_{i,j}^{k,q}$ as the binary variable with $y_{i,j}^{k,q} = 1$ indicating b_i's beam on channel k covers s_j when b_i's antenna beamwidth on channel k is of $q\theta_{\min}$.

$$\begin{aligned} x_{i,j}^{k,q} &\le y_{i,j}^{k,q} \\ x_{i,j}^{k,q} &\le t_i^{k,q} \end{aligned} \tag{2}$$

Now, we begin to build coverage relations between b_i and s_j on channel k determined by the antenna orientation φ_i^k when beamwidth $\theta_i^k = q\theta_{\min}$. It can be easily drawn as Figure 3. The corresponding mathematical equations are shown in (3) and (4). Let $\beta_{i,j}$ denote the angle measured counter-clockwise from the horizontal axis to the directional line from b_i to s_j. When $q\theta_{\min} \le \beta_{i,j}$, (3) is depicted by the thick lines in Figure 3(a). When $\beta_{i,j} \le q\theta_{\min}$, (4) is depicted by the thick lines in Figure 3(b).

$$y_{i,j}^{k,q} = \begin{cases} 0 & : \quad 0 \le \varphi_i^k < \beta_{i,j} - q\theta_{\min}; \\ 1 & : \quad \beta_{i,j} - q\theta_{\min} < \varphi_i^k \le \beta_{i,j}; \\ 0 & : \quad \beta_{i,j} \le \varphi_i^k < 2\pi; \end{cases} \tag{3}$$

$$y_{i,j}^{k,q} = \begin{cases} 1 & : \quad 0 \le \varphi_i^k < \beta_{ij}; \\ 0 & : \quad \beta_{i,j} \le \varphi_i^k < 2\pi + \beta_{i,j} - q\theta_{\min}; \\ 1 & : \quad 2\pi + \beta_{i,j} - q\theta_{\min} \le \varphi_i^k < 2\pi; \end{cases} \tag{4}$$

The relations between $y_{i,j}^{k,q}$ and φ_i^k are obviously nonlinear. In the following two cases, we shall show that these relations can be linearized [4].

- Case 1: $q\theta_{\min} \le \beta_{i,j}$

  From Figure 3(a), we can observe that $y_{i,j}^{k,q}$ can be linearly derived by two new binary variables $y_{i,j}^{k,q1}$ and $y_{i,j}^{k,q2}$, which are defined in (5) and (6).

$$y_{i,j}^{k,q1} = \begin{cases} 0 & : \quad 0 \le \varphi_i^k < \beta_{i,j} - q\theta_{\min}; \\ 1 & : \quad \beta_{i,j} - q\theta_{\min} \le \varphi_i^k < 2\pi; \end{cases} \tag{5}$$

$$y_{i,j}^{k,q2} = \begin{cases} 1 & : \quad 0 \le \varphi_i^k < \beta_{i,j}; \\ 0 & : \quad \beta_{i,j} \le \varphi_i^k < 2\pi; \end{cases} \tag{6}$$

Note that (5) and (6) are also depicted by thick lines in Figure 4(a) and (b), respectively. Because $y_{i,j}^{k,q}$ can be decomposed into $y_{i,j}^{k,q1}$ $y_{i,j}^{k,q2}$, we need to derive linear constraints for $y_{i,j}^{k,q1}$ and $y_{i,j}^{k,q2}$. A close look would lead us to the finding that the binary variables can be constrained by the quadrangles in Figure 4(a) and (b), respectively. Therefore, the decomposition of $y_{i,j}^{k,q}$ can be shown by (7).

$$\begin{aligned} y_{i,j}^{k,q} &= y_{i,j}^{k,q1} + y_{i,j}^{k,q2} - 1; \\ y_{i,j}^{k,q1} &\le \frac{1}{\beta_{i,j} - q\theta_{min}} \varphi_i^k; \\ y_{i,j}^{k,q1} &\ge \frac{1}{2\pi - \beta_{i,j} + q\theta_{\min}} \left(\varphi_i^k - \beta_{i,j} + q\theta_{\min} \right); \end{aligned}$$

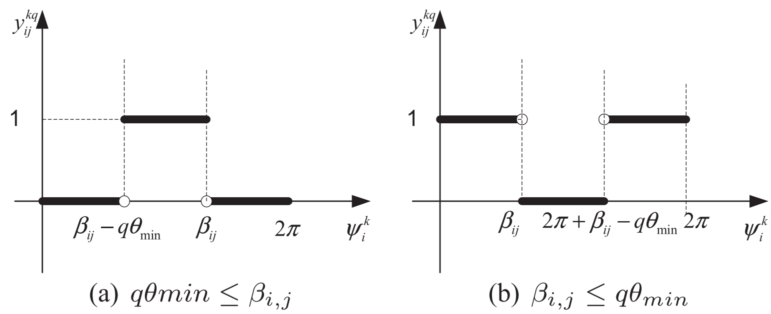

Figure 3. Two possible relations between $y_{i,j}^{k,q}$ and φ_i^k. (a) $q\theta_{\min} \le \beta_{i,j}$; (b) $\beta_{i,j} \le q\theta_{\min}$.

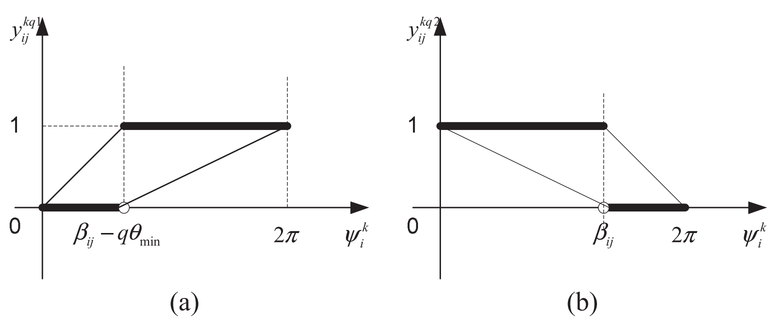

Figure 4. The decomposition of $y_{i,j}^{k,q}$ when $\theta_{\min} \le \beta_{i,j}$.

Wirel. Commun. Mob. Comput. 2015; **15**:260–275 © 2012 John Wiley & Sons, Ltd.
DOI: 10.1002/wcm

$$y_{i,j}^{k,q2} \geq \frac{-1}{\beta_{ij}}\left(\varphi_i^k - \beta_{i,j}\right);$$
$$y_{i,j}^{k,q2} \leq \frac{-1}{2\pi - \beta_{i,j}}\left(\varphi_i^k - 2\pi\right); \tag{7}$$

- Case 2: $q\theta_{\min} \geq \beta_{ij}$;

  From Figure 4, similarly, we can observe that $y_{i,j}^{k,q}$ can be linearly derived by two new binary variables $y_{i,j}^{k,q1}$ and $y_{i,j}^{k,q2}$, which are defined in (8) and (9).

$$y_{i,j}^{k,q1} = \begin{cases} 1 & : \quad 0 \leq \varphi_i^k < \beta_{ij}; \\ 0 & : \quad \beta_{ij} - q\theta_{\min} \leq \varphi_i^k < 2\pi; \end{cases} \tag{8}$$

$$y_{i,j}^{k,q2} = \begin{cases} 0 & : \quad 0 \leq \varphi_i^k < 2\pi + \beta_{i,j} - q\theta_{\min}; \\ 1 & : \quad 2\pi + \beta_{ij} - q\theta_{\min} \leq \varphi_i^k < 2\pi; \end{cases} \tag{9}$$

(8) and (9) are also depicted by thick lines in Figure 5(a) and (b), respectively.

Similarly, when $q\theta_{\min} \geq \beta_{i,j}$, the decomposition of $y_{i,j}^{k,q}$ can be shown by (10).

$$y_{i,j}^{k,q} = y_{i,j}^{k,q1} + y_{i,j}^{k,q2};$$
$$y_{i,j}^{k,q1} \geq \frac{-1}{\beta_{ij}}\left(\varphi_i^k - \beta_{i,j}\right);$$
$$y_{i,j}^{k,q1} \leq \frac{-1}{2\pi - \beta_{i,j}}\left(\varphi_i^k - 2\pi\right);$$
$$y_{i,j}^{k,q2} \leq \frac{1}{2\pi + \beta_{ij} - q\theta_{\min}}\varphi_i^k;$$
$$y_{i,j}^{k,q2} \geq \frac{1}{q\theta_{\min} - \beta_{i,j}}\left(\varphi_i^k - 2\pi - \beta_{i,j} + q\theta_{\min}\right); \tag{10}$$

3.2. Rate calculation

In this paper, we assume all BSs use the same transmit power P on all channels. The more complex issues of power control will be deferred for future research. Let us denote the link on channel k between BS b_i and SU s_j when the beamwidth of b_i's antenna is of $q\theta_{\min}$ as $l_{i,j}^{k,q}$. Let $d_{i,j}$ denote the physical distance between b_i and s_j. n denotes the path loss index. The received power of $l_{i,j}^{k,q}$ is denoted as $p_{i,j}^{k,q}$, which can be calculated using (11).

$$p_{i,j}^{k,q} = \frac{2\pi P}{q\theta_{\min} d_{i,j}^n} \tag{11}$$

The rate of link $l_{i,j}^{k,q}$, denoted as $c_{i,j}^{k,q}$, can be calculated as (12) based on (11).

N_0 denotes the ambient noise power, B denotes the number of BSs, N denotes the number of SUs. The term $\sum_{a=1}^{B}\sum_{b=1}^{N}\sum_{q=1}^{Q} t_a^{k,q} y_{a,j}^{k,q} p_{a,j}^{k,q}$ represents the interference power on channel k at s_j.

3.3. Interference constraints

For link $l_{i,j}^{k,q}$ to be reliable, we require that (13)

In practice, γ can be the minimum signal to interference and noise ratio (SINR) required to achieve a certain bit error rate performance at each SU. The value of γ depends on specific coding, modulation and detection schemes being employed.

$$c_{i,j}^{k,q} = log_2\left(1 + \frac{p_{i,j}^{k,q}}{N_0 + \sum_{a=1}^{B}\sum_{b=1,b\neq j}^{N}\sum_{q=1}^{Q} t_a^{k,q} y_{a,j}^{k,q} p_{a,j}^{k,q}}\right) \tag{12}$$

$$\frac{p_{i,j}^{k,q}}{N_0 + \sum_{a=1,a\neq i}^{B}\sum_{b=1}^{N}\sum_{q=1}^{Q} t_a^{k,q} y_{a,j}^{k,q} p_{a,j}^{k,q}} \geq \gamma \quad if \quad x_{i,j}^{k,q} = 1 \tag{13}$$

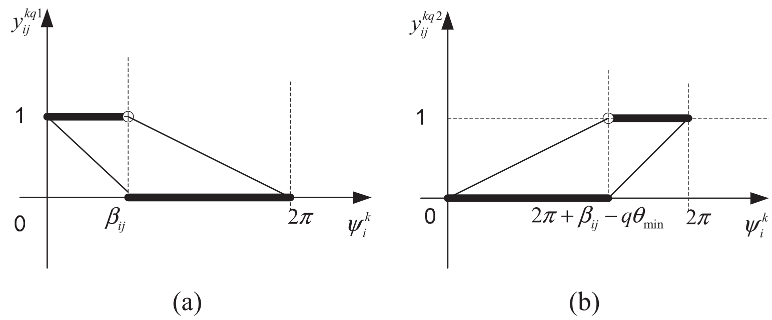

Figure 5. The decomposition of $y_{i,j}^{k,q}$ when $q\theta_{\min} \geq \beta_{ij}$.

Note that (13) can be transformed as (14).

$$x_{i,j}^{k,q}(\gamma N_0 + \lambda) + \gamma \sum_{a=1,a\neq i}^{B} \sum_{b=1}^{N} \sum_{q=1}^{Q} t_a^{k,q} y_{a,j}^{k,q} p_{a,j}^{k,q} - p_{i,j}^{k,q} \leq \lambda \tag{14}$$

where λ denotes a very large value.

3.4. Protecting primary users

To protect operations of PUs, we require that the interference power caused by all SUs on each channel is below a threshold value ζ, shown as follows:

$$\sum_{i=1}^{B} \sum_{q=1}^{Q} t_i^{k_{j*}q} y_{i,j*}^{k_{j*}q} p_{i,j*}^{k_{j*},q} \leq \zeta \forall j* \in \mathcal{P} \tag{15}$$

where k_{j*} denotes the index of the channel on which p_j is receiving signals. $y_{i,j*}^{k_{j*},q}$ denotes the binary variable with $y_{i,j*}^{k_* j,q} = 1$ indicating b_i's transmission beam on channel k_{j*} covers the jth PU p_j when the beamwidth of b_i's antenna is $q\theta_{\min}$. Let $p_{i,j*}^{k_{j*},q}$ denote the interference power on channel k_{j*} from b_i to p_j when the beamwidth of b_i's antenna is $q\theta_{\min}$. As (7) and (10), we then can derive determinant conditions (16) and (17) on $y_{i,j*}^{k_{j*},q}$ using $\varphi_i^{k_{j*}}$, $q\theta_{\min}$ and $\beta_{i,j*}$, which denotes the angle from the horizontal axis to the directional line from b_i to p_j.

- Case 1: $\beta_{i,j*} \geq q\theta_{\min}$

$$\begin{aligned}
&y_{i,j*}^{k_{j*},q} \leq y_{i,j*}^{k_{j*},q1} + y_{i,j*}^{k_{j*},q2} - 1;\\
&y_{i,j*}^{k_{j*},q1} \leq \frac{1}{\beta_{i,j*} - q\theta_{\min}} \varphi_i^{k_{j*}};\\
&y_{i,j*}^{k_{j*},q1} \geq \frac{1}{2\pi - \beta_{i,j*} + q\theta_{\min}} \left(\varphi_i^{k_{j*}} - \beta_{i,j*} + q\theta_{\min}\right);\\
&y_{i,j*}^{k_{j*},q2} \geq \frac{-1}{\beta_{i,j*}} \left(\varphi_i^{k_{j*}} - \beta_{i,j*}\right);\\
&y_{i,j*}^{k_{j*},q2} \leq \frac{-1}{2\pi - \beta_{i,j*}} \left(\varphi_i^{k_{j*}} - 2\pi\right);
\end{aligned} \tag{16}$$

- Case 2: $\beta_{ij*} \leq q\theta_{\min}$

$$\begin{aligned}
&y_{i,j*}^{k_{j*},q} \leq y_{i,j*}^{k_j,q1} + y_{i,j*}^{k_{j*},q2};\\
&y_{i,j*}^{k_{j*},q1} \geq \frac{-1}{\beta_{i,j*}} \left(\varphi_i^{k_{j*}} - \beta_{i,j*}\right);\\
&y_{i,j*}^{k_{j*},q1} \leq \frac{-1}{2\pi - \beta_{i,j*}} \left(\varphi_i^{k_{j*}} - 2\pi\right);\\
&y_{i,j*}^{k_{j*},q2} \leq \frac{1}{2\pi + \beta_{i,j*} - q\theta_{\min}} \varphi_i^{k_{j*}};\\
&y_{i,j*}^{k_{j*},q2} \geq \frac{1}{q\theta_{\min} - \beta_{i,j*}} \left(\varphi_i^{k_{j*}} - 2\pi - \beta_{i,j*} + q\theta_{\min}\right);
\end{aligned} \tag{17}$$

3.5. Objective

Recall that the objective of the ADCA problem is to maximize the sum rate achieved by all SUs, which can be formulated as (18).

$$max \quad \sum_{i=1}^{B} \sum_{j=1}^{N} \sum_{k=1}^{C} \sum_{q=1}^{Q} x_{i,j}^{kq} c_{i,j}^{k,q} \tag{18}$$

where C denotes the number of channels.

Remark: In this paper, we assume the channel usage pattern for PUs is fairly static. With the objective of maximizing the overall throughput, the optimal solution to the configuration of CRN, in terms of antenna orientation, beamwidth and channel assignment, tends to be static. Therefore, it is not necessary to introduce scheduling in a slotted time system to the formulation.

4. DESIGN OF A GREEDY ALGORITHM

In this section, we present a greedy algorithm. This algorithm increases the sum rate of CRN iteratively until it can not be increased. The main idea is presented in Section 4.2, which includes maximum throughput estimation, BS sorting and channel usage implementation. The details of each module is described in Section 4.3.

4.1. Intuition

The main difficulty for the ADCA problem lies in the objective function as (18), where $c_{i,j}^{k,q}$ is a nonlinear term with $x_{i,j}^{k,q}$ and $y_{i,j}^{k,q}$ in the denominator contained in a logarithmic function. It is obviously very hard to approximate the optimal solution via relaxing the objective function. Then, we realize the variables $x_{i,j}^{k,q}$ and $y_{i,j}^{k,q}$ in the objective function represents interference power from multiple BSs. If we divide the large optimization task and distribute subtasks to each BS heuristically, the objective function for each smaller optimization problem would be much easier in the sense that interference from only one BS is considered during one iteration.

4.2. Description of the greedy algorithm

Our greedy algorithm increases the overall network throughput iteratively and terminates until the overall network throughput can not be increased further. We assume that each BS maintains one database recording position information of all PUs and SUs, current channel assignment, antenna orientation and beamwidth, named as Table of Assignment Links (TAL). At the beginning of an iteration, each BS pretends that the existing links that connect itself are annihilated. Then each BS proceeds calculating the best possible throughput increase under the interference constraints imposed by both PUs and existing links

Wirel. Commun. Mob. Comput. 2015; **15**:260–275 © 2012 John Wiley & Sons, Ltd.
DOI: 10.1002/wcm

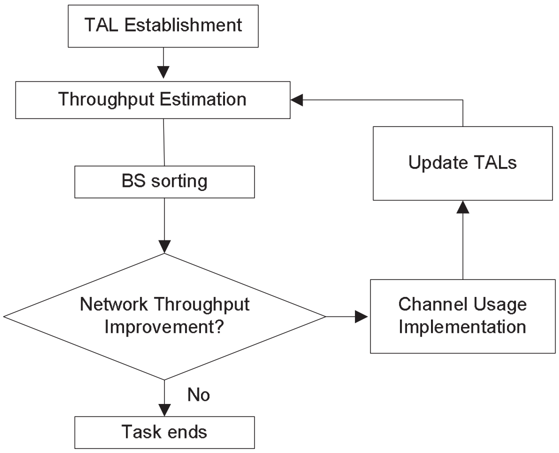

Figure 6. The flow chart showing how our greedy algorithm works.

within the CRN. After calculating the potentially maximum throughput increase, each BS exchanges its result with other BSs, and finally, the globally largest is identified as associated with one BS. Then, the chosen BS is required to implement its channel assignment, antenna orientation and beamwidth to best increase the overall network throughput. At the last step of each iteration, new results of assigned links should be updated in the TALs of all BSs. The basic diagram of our greedy algorithm is shown in Figure 6.

The notation used in this section is listed in Table II.

4.3. Details of each module

4.3.1. Table of assignment links establishment.

We first present the method of TAL establishment. For each BS, the TAL records updated information of the positions of PUs and SUs, channel usage pattern, antenna orientation and associated beamwidth all over CRN. The information in TAL will help each BS avoid failing existing links and impacting PUs by generating excessive interference while establishing new links.

4.3.2. Maximum throughput estimation.

We now present the method for each BS to bring the largest increase to the sum rate performance. As the BS is trying to update the setting of beams on each channel,

Table II. Notation.

Symbol	Definitions
$x_j^{k,q}$	Binary variable indicating the assignment of the current BS to s_j on channel k of beamwidth $q\theta_{\min}$
$y_j^{k,q}$	Binary variable indicating the current BS covers s_j on channel k of beamwidth $q\theta_{\min}$
$y_{j*}^{k_{j*},q}$	Binary variable indicating the current BS covers p_j on channel k_{j*} of beamwidth $q\theta_{\min}$
β_j	The counter-clockwise angle of the line from the current BS to s_j
φ_k	The counter-clockwise angle of the beam on channel k of the current BS
t_k^q	Binary variable indicating if the current BS's beam on channel k has beamwidth $q\theta_{\min}$
$\mathcal{E}$	The set of existing links
$p_j^{k,q}$	The received power at s_j from current BS when t_k^q=1
$p_{j*}^{k_{j*},q}$	The received power at p_j from current BS when $t_{k_{j*}}^q$=1
β_{j*}	Then counter-clockwise angle of the line from current BS to p_j
i_l	The index of BS of the lth existing link
j_l	The index of SU of the lth existing link
k_l	The channel of the lth existing link
$q_l\theta_{\min}$	The beamwidth of the lth existing link
I_j^k	The overall interference power of the assigned links at s_j on the kth channel
I_{j*}	The overall interference power of the assigned links at p_j on the k_{j*}th channel
$c_j^{k,q}$	The rate of the link between the current BS and s_j
c_l	The rate of the lth existing link
$\mathcal{P}$	The set of all PUs
$\mathcal{R}$	The set of SUs not connected to BSs

BS, base stations; SU, secondary user; PU, primary user.

it should be aware of increasing interference to existing links. Therefore, the achievable rate on other links would be probably deteriorated. Moreover, hypothetically annihilating all the associated links, the BS should also take into account the interference from existing links when establishing new connections.

- Preliminaries: let $x_j^{k,q}$ denote the binary assignment variable indicating the s_j is connected with the current BS at channel k of which the beamwidth is $q\theta_{\min}$. Let $y_j^{k,q}$ denote the binary coverage variable indicating s_j is covered by the current BS at channel k of which the beamwidth is $q\theta_{\min}$. β_j denotes the angle measured counter-clockwise from the horizontal axis to the directional line from the current BS to s_j. φ_k denotes the angle measured counter-clockwise from horizontal axis to the first side of the beam on the kth channel of the current BS. We introduce a binary variable t_k^q indicating if the current BS's beam on channel k has beamwidth $q\theta_{\min}$ when $t_k^q = 1$. Obviously, it is required that $\sum_{q=1}^{Q} t_k^q \leq 1 \forall k$. Similar as (2), we have the following:

$$\begin{aligned} x_j^{k,q} &\leq y_j^{k,q} \\ x_j^{k,q} &\leq t_k^q \end{aligned} \tag{19}$$

As a note, $y_j^{k,q}$ is decided by β_j and φ_k similarly as (3) and (4), which can be mathematically formulated as a linear constraint as in Section 3.1.

- Protecting existing links: we first introduce some notation. Let us denote the received power at s_j from the current BS on channel k when the antenna's beamwidth is $q\theta_{\min}$ as $p_j^{k,q}$. We use $\mathcal{E}$ to denote the set of existing links. Let i_l, j_l, k_l denote the index of the BS, SU and channel of the lth existing link, respectively. The beamwidth of the lth existing link is of $q_l\theta_{\min}$. I_j^k denotes the overall interference power of the assigned links at s_j on the kth channel. We then denote the set of existing links as $\mathcal{E}$. The value of $p_j^{k,q}$ can be easily calculated on the basis of (11). From (13), we can obtain the following constraint (20) to protect existing links against excessive interference.

$$\begin{aligned} &\gamma \left(\sum_{q=1}^{Q} p_{j_l}^{k_l,q_l} y_{j_l}^{k_l,q_l} t_{k_l}^{q_l} + N_0 + I_{j_l} \right) \\ &\leq p_{i_l,j_l}^{k_l,q_l}, \forall l \in \mathcal{E} \end{aligned} \tag{20}$$

As a note, the nonlinear term $y_{j_l}^{k_l,q_l} t_{k_l}^{q_l}$ can be substituted by a binary variable $u_{j_l}^{k_l,q_l}$ and then linearized as follows:

$$\begin{aligned} y_{j_l}^{k_l,q_l} + t_{k_l}^{q_l} &\geq 2u_{j_l}^{k_l,q_l} \\ y_{j_l}^{k_l,q_l} + t_{k_l}^{q_l} - u_{j_l}^{k_l,q_l} &\leq 1 \end{aligned} \tag{21}$$

- Interference constraint for new links: as (13), the SINR at the receiver end should be larger than γ for newly established links, which is shown as follows:

$$p_j^{k,q} \geq \gamma \left(N_0 + I_j^k \right) x_j^{k,q} \qquad \forall j \in \mathcal{R} \tag{22}$$

where $\mathcal{R}$ represents the set of SUs without connections.

- Protecting primary users: for ease of demonstration, we first introduce some notation. k_{j*} denotes the index of the channel on which p_j is operating. I_{j*} denotes the overall interference power of the assigned links at p_j at the k_{j*}th channel. β_{j*} denotes the angle measured counter-clockwise from the horizontal axis to the directional line from the current BS to p_j. The received power at p_j from the current BS on channel k of beamwidth $q\theta_{\min}$ is denoted as $p_{j*}^{k_{j*},q}$. Obviously, the value of $p_{j*}^{k_{j*},q}$ can be easily calculated on the basis of (11). The set of all PUs is denoted as $\mathcal{P}$. $y_{j*}^{k_{j*},q}$ denotes the binary coverage variable indicating if the current BS is covering p_j at beamwidth of $q\theta_{\min}$. $p_{j*}^{k_{j*},q}$ denotes the received power of the current BS on the k_{j*}th channel when the beamwidth is $q\theta_{\min}$ at p_j.

$$\sum_{q=1}^{Q} p_{j*}^{k_{j*},q} t_{k_{j*}}^q y_{j*}^{k_{j*},q} + I_{j*} \leq \zeta \qquad \forall j* \in \mathcal{P} \tag{23}$$

As a note, $y_{j*}^{k_{j*},q}$ is decided by β_{j*} and $\varphi_{k_{j*}}$ similarly as (3) and (4), which can be mathematically formulated as a linear constraint as in Section 3.1. In addition, the term $t_{k_{j*}}^q y_{j*}^{k_{j*},q}$ can be substituted by a new variable $v_{j*}^{k_{j*},q}$ and then linearized as follows:

$$\begin{aligned} t_{k_{j*}}^q + y_{j*}^{k_{j*},q} &\geq 2v_{j*}^{k_{j*},q} \\ t_{k_{j*}}^q + y_{j*}^{k_{j*},q} - v_{j*}^{k_{j*},q} &\leq 1 \end{aligned} \tag{24}$$

- Rate calculation: we use $c_j^{k,q}$ to denote the rate of the link between s_j and the current BS on channel k when the antenna beamwidth is $q\theta_{\min}$, which can be calculated as follows:

$$c_j^{k,q} = log_2 \left(1 + \frac{p_j^{k,q}}{N_0 + I_j^k} \right) \qquad \forall j \in \mathcal{R}; \tag{25}$$

Note that the rate of the existing links could probably be reduced because of newly introduced interference. $\forall l \in \mathcal{E}$, its rate c_l can be changed to $c_l^{k_l,q}$ if $y_{j_l}^{k_l,q} t_{k_l}^q = 1$, which is calculated as follows:

$$c_l^{k_l,q} = log_2 \left(1 + \frac{p_{i_l,j_l}^{k_l,q_l}}{N_0 + I_{j_l}^{k_l} + p_{j_l}^{k_l,q}} \right); \tag{26}$$

Wirel. Commun. Mob. Comput. 2015; **15**:260–275 © 2012 John Wiley & Sons, Ltd.
DOI: 10.1002/wcm

- Objective function: recall that the greedy algorithm iteratively increases the network throughput, thus the BS should try to maximize the sum rate of newly established links as well as probably deteriorated existing links, which can be mathematically stated as (27).

$$\begin{aligned} max \quad & \sum_{j\in\mathcal{R}}\sum_{k=1}^{C}\sum_{q=1}^{Q} x_j^{k,q} c_j^{k,q} + \\ & \sum_{l\in\mathcal{E}}\left(y_{jl}^{k_l,q} t_{k_l}^{q} c_l^{k_l,q} + \left(1-y_{jl}^{k_l,q} t_{k_l}^{q}\right) c_l\right) \end{aligned} \tag{27}$$

It should be noted that the nonlinear term $y_{jl}^{k_l,q} t_{k_l}^{q}$ can be linearized as (24).

Putting together the objective and all the constraints described earlier, we formulate a MILP problem, which can be solved by the branch and bound algorithm.

4.3.3. Base station sorting.

This module is aimed to identify the BS, which can bring the maximum throughput benefit, and hence, the network throughput can be increased greedily. After each BS is associated with a maximum throughput, they can exchange their results with neighboring BSs in a distributed fashion. At the end of this process, each BS should keep the maximum network throughput along with the ID of the BS that produces this amount.

The implementation of this module entails a certain amount of information exchange. Once a BS receives its knowingly best network throughput, it propagates this datum to its neighboring BSs exactly once. In particular, each BS is only concerned if its maximum network throughput is larger than any other BS in this iteration. Thus, they would discard their own maximum network throughput along with the associated beam configuration once they realize some other BS produces larger throughput. For the case of equal throughput, the BS would also discard its own results if the BS that produces the same amount of throughput is indexed smaller. This sorting procedure terminates when any BS has not been notified of any larger throughput for a preset amount of time.

4.3.4. Channel usage implementation.

Finally, we discuss the method of channel usage implementation and TAL updating. At first, this module is applied at the BS whose maximum throughput is the largest among all BSs in each iteration. The BS updates the calculated channel assignment, antenna orientation and beamwidth in its TAL. This BS also has to inform other BSs to update their TALs for calculating the maximum throughput during the next iteration.

4.4. Proof of convergence

We now show that the algorithm must converge. We show that in each iteration, the algorithm increases the throughput performance of CRN. Because the overall throughput is upper bounded, this implies that the algorithm must converge.

At the beginning of each iteration, each BS's beam configuration represents a feasible solution to the maximum throughput estimation problem formulated in Section 4.3.2. After solving the maximum throughput estimation problem, we obtain the optimal solution for each BS. Therefore, no matter which BS is chosen to implement new settings for antenna orientation and beamwidth, the network throughput is expected to grow larger than the lower bound at the beginning of the iteration.

Because the network throughput performance monotonically increased after every iteration, convergence of the greedy algorithm is guaranteed.

4.5. Complexity analysis

The complexity analysis of the greedy algorithm is presented as follows. During each iteration, the majority computation mainly resides in the step of maximum throughput estimation. The solution space contains all combinations of binary variables and continuous variables. The binary variables include $x_j^{k,q}, y_j^{k,q}, y_{j*}^{k_{j*},q}, t_k^q$ (as explained in Table II), which totals as many as $(N \times C \times Q + N \times C \times Q + |\mathcal{P}|^2 \times Q + C \times Q)$. The continuous variables include φ_k, which contains at most C variables. The MILP problem can be solved by branch and bound algorithm, which could potentially search all 2^L solutions, where L denotes the number of binary variables. Therefore, the running time for the greedy algorithm for one iteration equals to $O(2^{(2N+1)CQ+|\mathcal{P}|^2 Q})$. As all BSs are required to compute the MILP problem in one iteration, and the total number of iterations is measured as $O(B)$, the total times to solve the MILP algorithm can be approximated as $O(B^2)$. Therefore, the overall computation complexity for the greedy scheme can be approximated as $O(B^2 2^{(2N+1)CQ+|\mathcal{P}|^2 Q}) = O(2^{(2N+1)CQ+|\mathcal{P}|^2 Q})$.

4.6. Notes on implementation issue

During the first few iterations, the majority of SUs can be connected with only one BS under many circumstances. One of them is that each BS has abundant beams and large beamwidth such that most SUs can be covered to achieve high network throughput. The other one is that the number of SUs is comparatively small and they are not far away from one BS. When one BS is covering most of the SUs, these links are protected as existing links in future iterations, which would cause the greedy algorithm to converge very fast. To avoid this situation, we impose different procedures at the beginning of the greedy algorithm: the set SUs are divided into B clusters according to their distances to the BSs; then, each BS sequentially estimates the maximum throughput and implement the result considering the cluster of SUs to which the current BS is the nearest.

4.7. Other algorithm

Because the existing schemes can not be directly applied to solve the ADCA problem, we design an Reformulation-Linearization Technique (RLT)-based heuristic scheme to compare with the proposed greedy scheme. RLT[24] has been widely used to solve non-linear optimization problems. Because the ADCA problem is a non-linear optimization problem, involving both integer and non-integer variables, the RLT technique can be employed to relax the original problem to linear form and obtain the non-integer variables. Then, on the basis of acquired solution for non-integer variables, a greedy scheme is employed to obtain the solution for integer variables. Specifically, $t_a^{k,q} y_{a,j}^{k,q}$ in (14) and $t_i^{k_{j*},q} y_{i,j}^{k_{j*},q}$ in (15) are polynomial terms. By using RLT, we can substitute these terms with new variables, thus relaxing nonlinear terms into linear terms. For instance,

$$
\begin{aligned}
&t_i^{k_{j*},q} + y_{i,j*}^{k_{j*},q} - w_i^{k_{j*},q} \le 1 \\
&t_i^{k_{j*},q} + y_{i,j*}^{k_{j*},q} \ge 2w_i^{k_{j*},q}
\end{aligned}
\tag{28}
$$

Moreover, we can relax (12) as follows:

$$
c_{i,j}^{k,q} = log_2\left(1 + \frac{p_{i,j}^{k,q}}{N_0}\right); \tag{29}
$$

After relaxation, we can obtain the upper bound by solving a linear programming problem. We fix the non-integer variables $\varphi_i^k (1 \le i \le B, 1 \le k \le C)$ and employ the following heuristic algorithm to solve the assignment variables $\mathbf{X}$. The heuristic algorithm increases the overall network throughput iteratively and terminates until the overall network throughput can not be further increased. At the beginning of an iteration, each BS pretends that the existing links that connect itself are annihilated. Then, each BS proceeds calculating the best possible throughput increase under the interference constraints imposed by both PUs and existing links within the CRN. After calculating the potentially maximum throughput increase, each BS exchanges its result with other BSs, and finally, the globally largest is identified associated with one BS. Then, the chosen BS is required to implement its channel assignment, antenna orientation and beamwidth to best increase the overall network throughput. At the last step of each iteration, new results of assigned links should be broadcasted to all BSs. One BS solves the following binary integer programming problem during one iteration. Note that $y_{j_l}^{k_l,q_l}$, $y_{j*}^{k_{j*},q}$ and $y_j^{k,q}$ are all known because angle of beams on each BS are fixed. The objective is the same as (27), and constraints are extracted from (19), (20), (23) and (22).

$$
\begin{aligned}
Max \quad & \textstyle\sum_{j\in\mathcal{R}} \sum_{k=1}^{C} \sum_{q=1}^{Q} x_j^{k,q} c_j^{k,q} + \\
& \textstyle\sum_{l\in\mathcal{E}} \left(y_{j_l}^{k_l,q} t_{k_l}^{q} c_l^{k_l,q} + \left(1 - y_{j_l}^{k_l,q} t_{k_l}^{q}\right) c_l \right) \\
s.t \quad & \\
& \textstyle\sum_{q=1}^{Q} t_k^q \le 1 \\
& x_j^{k,q} \le y_j^{k,q} \quad \forall j \in \mathcal{R} \\
& x_j^{k,q} \le t_k^q \quad \forall j \in \mathcal{R} \\
& \gamma \left(\textstyle\sum_{q=1}^{Q} p_{j_l}^{k_l,q_l} y_{j_l}^{k_l,q_l} t_{k_l}^{q_l} + N_0 + I_{j_l} \right) \\
& \quad \le p_{i_l,j_l}^{k_l,q_l}, \forall l \in \mathcal{E} \\
& \textstyle\sum_{q=1}^{Q} p_{j*}^{k_{j*},q} t_{k_{j*}}^{q} y_{j*}^{k_{j*},q} + I_{j*} \\
& \quad \le \zeta \quad \forall j* \in \mathcal{P} \\
& p_j^{k,q} \ge \gamma \left(N_0 + I_j^k \right) x_j^{k,q} \qquad \forall j \in \mathcal{R} \\
& 1 \le k \le C, 1 \le q \le Q
\end{aligned}
\tag{30}
$$

5. PERFORMANCE EVALUATION

In this section, we present simulation results to demonstrate the performance of our greedy algorithm. Ideally, the best performance measure of our distributed optimization algorithm is the solution to the centralized optimization problem. However, as is shown in the Appendix section, the problem formulation is in the form of MINLP and is NP-hard. Although the exact solution to the MINLP problem is not obtainable, we are able to develop a tight upper bound for the objective function of the problem. As a result, we will compare the performance of our greedy algorithm with the upper bound.

5.1. Simulation setup

We consider a square service area of size 100 km $\times$ 100 km in which a CRN is deployed. Three BSs are placed at the coordinates $\{[3, 4]; [4, 7]; [7, 4]\} \times 10^4$. Fifteen SUs and five PUs are randomly deployed within the service area. We assume a free-space path loss model with the path-loss exponent $n = 2$. The ambient noise power at each PU and SU is $N_0 = -100$ dB. The channel bandwidth is of 1 MHz. The threshold power for PUs is $\zeta = -90$ dB. We arbitrarily set the channels where PUs are receiving signals. For each set of system parameters, we generate 20 instances of the network scenarios with randomly distributed user nodes to obtain the average performance.

5.2. Evaluation metric

To evaluate the performance of the greedy algorithm, the metric we utilize is the average throughput of CRN over the 20 instances of different network scenarios.

Wirel. Commun. Mob. Comput. 2015; **15**:260–275 © 2012 John Wiley & Sons, Ltd.
DOI: 10.1002/wcm

5.3. Simulation results

(1) Impact of transmit power: We evaluate the impact of transmit power on the performance of the CRN. Figure 7 shows the performance comparison when we change the transmit power from 0.2 to 1 W. Because the optimal performance lies between the feasible solution via the greedy algorithm and the upper bound, it is obvious that the throughput performance of the greedy algorithm produces near-optimal solution. Besides, as the transmit power increases from 0.2 to 1 W, the performance yielded by both the greedy algorithm and the upper bound increases, which agrees with the rate model (12). In addition, by comparing with the RLT-based scheme, the proposed greedy algorithm demonstrates very good performance.

(2) Impact of minimal beamwidth: Next, we look into the impact of minimal beamwidth $\theta_{\min}$ on the throughput performance of CRN. From Figure 8, it can be drawn that the greedy algorithm produces close-to-optimal performance. Moreover, we can see that the average performance for both via the greedy algorithm and the upper bound degrade as $\theta_{\min}$ increases. The reason lies in the fact that the received power of each link is inversely proportional to the beamwidth. As a result, the rate of each link is reduced because of the increase of $\theta_{\min}$ on the basis of the rate model (12). By comparing the performance of the proposed greedy algorithm with the RLT-based approach, it can be seen clearly that our proposed greedy scheme outperforms the RLT-based approach.

(3) Impact of interference threshold: In Figure 9, we evaluate the impact of interference threshold on the performance of the CRN. We can make two observations: first, the upper bound is close to the optimal performance; second, the greedy algorithm produces near-optimal performance. Besides, as the interference threshold γ increases from 30 to 50, both performances yielded by the greedy algorithm and the upper bound decrease. The rationale behind is that with higher interference threshold, less links would be able to succeed. In addition, our proposed greedy algorithm generates much smaller gap between its performance and upper bound than the RLT-based algorithm.

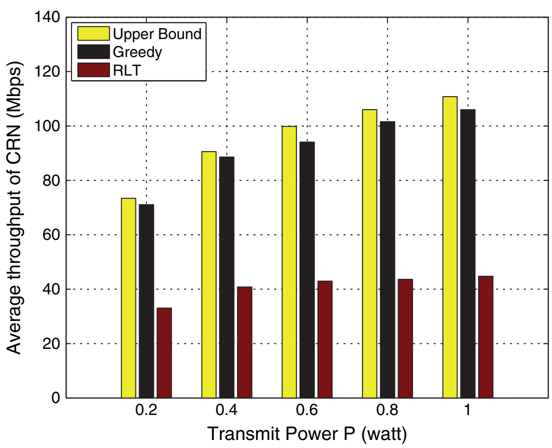

Figure 7. Simulation results when P changes. Twenty random-generated network topologies are tested for each parameter set.$\theta_{\min} = \pi/4$. $\gamma = 10$, $Q = 3$. C=3.

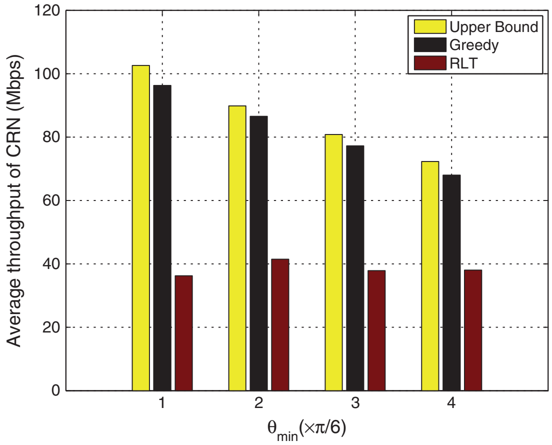

Figure 8. Simulation results when $\theta_{\min}$ changes. Twenty random-generated network topologies are tested for each parameter set. $\gamma = 10$, $Q = 3$, $P = 0.5$ W,C=3.

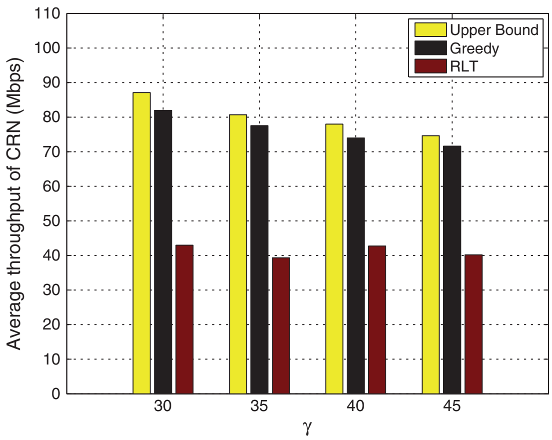

Figure 9. Simulation results when γ changes. Twenty random-generated network topologies are tested for each parameter set.$\theta_{\min} = \pi/4$. $p = 0.5$ W, $q = 3$. $c = 3$.

(4) Impact of Q: Then, we look into the impact of the number of angles Q on the throughput performance in Figure 10. From Figure 10, it is clear that the average of both of the performances yielded by the greedy algorithm and the upper bound increase when we change Q from 1 to 4. This is because more number of angles would give rise to more opportunities that one beam covers more SUs, which thereby increases the total throughput performance. This phenomenon demonstrates the advantage of variable beamwidth of directional antennas in network throughput of multicast communication (for unicast communication, the optimal solution usually consists of beams with minimal angle to maximize throughput). Furthermore, we can

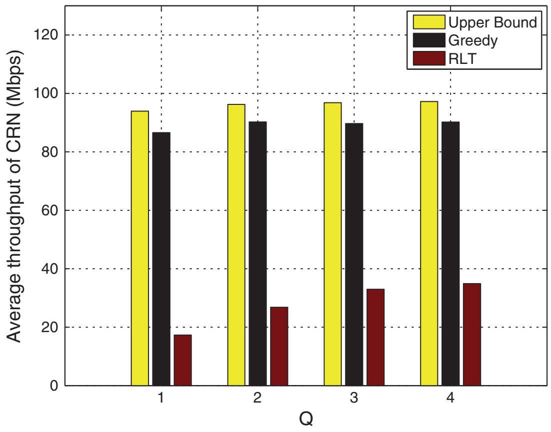

Figure 10. Simulation results when Q changes. Twenty random-generated network topologies are tested for each parameter set. $\theta_{\min} = \pi/8$. $P = 0.5$ W, $\gamma = 10$, $C = 2$.

see that the proposed greedy algorithm outperforms the RLT-based algorithm.

6. IMPACT OF POWER THRESHOLD FOR PUs:

As for the impact of power threshold ζ for PUs, we carry out numerical investigation in Figure 11. From Figure 11, first of all, the greedy algorithm yields performance close to the upper bound. In addition, we can see a slight increase as the threshold power increases from -90 to -50 db for the performance of the greedy algorithm. This is because the constraint of protecting the PUs is relaxed as ζ increases. In particular, as the constraint (23) shows, when ζ is enlarged, more interference to each PU is

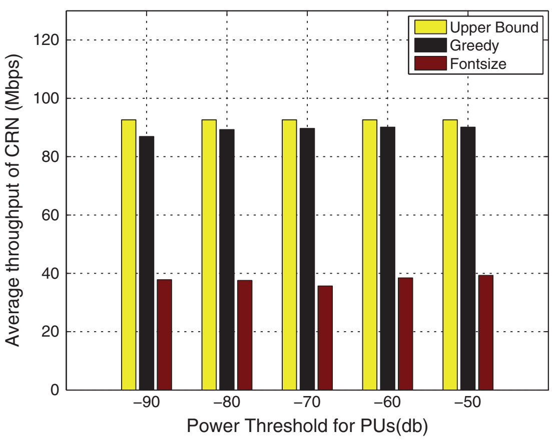

Figure 11. Simulation results when ζ changes. Twenty random-generated network topologies are tested for each parameter set. $\theta_{\min} = \pi/4$. $P = 0.5$ W, $Q = 3$, $\gamma = 10$.

allowed from CRNs, which leads to more possible establishment of secondary links or larger transmit power of individual downlink secondary connections. Therefore, the overall throughput of the cognitive network is increased. Besides, the proposed greedy algorithm yields much better performance than the RLT-based approach.

7. DISCUSSION

Although the current network model assumes that the channel usage pattern remains static, the proposed algorithm can be easily extended to handle the case when PUs dynamically change their channel usage pattern. We assume when PUs update operating channels, the BSs in CRN can sense which PUs have moved to which channels. Because each BS maintains one database recording position information of all PUs and SUs, current channel assignment, antenna orientation and beamwidth, they can update the channel usage pattern information accordingly. Therefore, each BS checks if its supported downlink multicast connections have caused interference to the PUs who newly updated their operating channel. The proposed greedy algorithm can be implemented involving only the BSs that have caused interference to PUs due to their dynamic channel usage. In particular, each BS pretends that the existing links that connect itself are annihilated. Then, each BS proceed in calculating the best possible throughput increase under the interference constraints imposed by both PUs with updated channel usage and existing links within the CRN. After calculating the potentially maximum throughput increase, each BS exchanges its result with other BSs, and finally, the globally largest is identified as associated with one BS. Then the chosen BS is required to implement its channel assignment, antenna orientation and beamwidth to best increase the overall network throughput. At the last step of each iteration, new results of the assigned links should be updated in the TALs of all BSs. With PUs dynamically changing channel usage pattern, all the approaches would be extended to apply in time dimension. Thus, results are also time-based. Until a specific time, the proposed greedy algorithm still keeps increasing the overall throughput performance iteratively every time after sensing channel usage change from the primary network. The adaptation to the CRN is incremental by implementing the greedy algorithm. In contrast, the RLT-based approach has to tear down all connections and rebuild them again once interference is caused to primary network due to channel usage update, which is very expensive. Besides, if scrutinized after a random primary network change of channel usage pattern, the greedy algorithm works by the same token as if the channel usage pattern were static among PUs. Therefore, given a specific time, the greedy algorithm should still yield performance that is relatively close to upper bound performance and much better than RLT-based approach.

Wirel. Commun. Mob. Comput. 2015; **15**:260–275 © 2012 John Wiley & Sons, Ltd.
DOI: 10.1002/wcm

In real applications, different BSs usually exert different transmit power levels in CRNs. Although BSs use identical transmit power for secondary downlink connections in the proposed network model, the greedy algorithm can be easily be applied to scenarios where BSs use different transmit power. Transmit powers play their role in the second step of greedy algorithm, when each BS calculates its biggest throughput increase. Because this step is implemented by each BS independently, different transmit powers on BSs will not cause any effect to the procedure of the BS's execution. Therefore, it is safe to claim that the proposed greedy algorithm is seamlessly applicable to CRNs where BSs use different transmit power levels. The results of proposed method would change though. Each BS would generate new throughput values with transmit power changed. Although it is hard to predict the change of the final absolute performance for the greedy algorithm with BSs using different transmit powers, the greedy algorithm should still yield performance that is close to the upper bound and much better than the RLT-based approach. The reason lies in the fact that the change of BSs' transmit powers will only affect the performance amplitudes of all approaches to the same extent and keep their relative performance unchanged. The impact of the parameters on the approaches described in Section 5 should remain valid.

The current network model assumes homogeneous SUs in CRNs. It is worth noting that the proposed greedy algorithm can easily address heterogeneous SUs in CRNs. In particular, each BS will maintain one database recording position information of all PUs and SUs, current channel assignment, antenna orientation and beamwidth, as well as SINR threshold of all SUs. When calculating the maximal throughput increase during the greedy algorithm, each BS modifies constraint (22) using the SINR threshold value based on the current SU, which the constraint applies to. By incorporating the modified constraint (22), each BS can calculate the potentially maximal throughput increase. After calculating the potentially maximum throughput increase, each BS exchanges its result with other BSs, and finally, the globally largest is identified as associated with one BS. Then the chosen BS is required to implement its channel assignment, antenna orientation and beamwidth to best increase the overall network throughput.

8. CONCLUSION

In this paper, we presented a study on multicast communications in CRN using directional antennas. We develop a mathematical model for such problem with joint consideration of ADCA. The main contribution of this paper is the development of a greedy optimization algorithm that iteratively increases the overall CRN network throughput. Simulation results show that the achievable performance via our greedy algorithm is close to the upper bound and also outperforms the RLT-based approach. Because the unknown optimal solution lies between the upper bound and the lower bound (feasible solution obtained via our greedy algorithm), we conclude that the results obtained by the greedy algorithm are very close to the optimal solution. Besides, it can also be drawn that the upper bound is very tight.

APPENDIX A: ANTENNA DIRECTIONALITY AND CHANNEL ASSIGNMENT PROBLEM FORMULATION AND UPPER BOUND

To develop a performance benchmark for the greedy algorithm, we first formulate the cross-layer optimization problem. Putting together all the constraints described in Section 3, we have the formulation (A.1). The optimization problem is in the form of MINLP, which is NP-hard in general. Because we are not able to obtain the exact solution, we develop an upper bound to this problem, which can be used as a measure for the performance of the greedy algorithm.

$$
\begin{aligned}
& max \textstyle\sum_{i=1}^{B} \sum_{j=1}^{N} \sum_{k=1}^{C} \sum_{q=1}^{Q} x_{i,j}^{k,q} c_{i,j}^{k,q} \\
& \textstyle\sum_{q=1}^{Q} t_i^{k,q} \le 1 \\
& x_{i,j}^{k,q} \le y_{i,j}^{k,q} \\
& x_{i,j}^{k,q} \le t_i^{k,q} \\
& x_{i,j}^{k,q} (\gamma N_0 + \lambda) + \gamma \textstyle\sum_{a=1}^{B} \sum_{b=1, b\neq j}^{N} \sum_{q=1}^{Q} p_{a,j}^{k,q} t_a^{k,q} y_{a,j}^{k,q} \\
& \qquad - p_{ij}^{kq} \le \lambda \\
& \textstyle\sum_{i=1}^{B} \sum_{q=1}^{Q} t_i^{k_{j*},q} y_{ij*}^{k_{j*},q} p_{i,j*}^{k_{j*},q} \le \zeta \\
& c_{i,j}^{k,q} = log_2 \left(1 + \frac{p_{i,j}^{k,q}}{N_0 + \sum_{a=1, a\neq i}^{B} \sum_{b=1}^{N} \sum_{q=1}^{Q} t_a^{k,q} y_{a,j}^{k,q} p_{a,j}^{k,q}} \right) \\
& (7)\ if\ \ \beta_{i,j} \ge q\theta_{\min},\ or\ (10)\ if\ \ \beta_{i,j} \le q\theta_{\min} \\
& (16)\ if\ \ \beta_{i,j*} \ge q\theta_{\min},\ or\ (17)\ if\ \ \beta_{i,j*} \le q\theta_{\min} \\
& x_{i,j}^{k,q}, y_{i,j}^{k,q}, y_{i,j}^{k,q1}, y_{i,j}^{k,q2}, y_{i,j*}^{k,q}, y_{i,j*}^{k,q1}, y_{i,j*}^{k,q2}, t_i^{k,q} \in \{0,1\} \\
& 1 \le i \le B, 1 \le j \le N, 1 \le k \le C, 1 \le q \le Q \\
& \forall j* \in \mathcal{P}, 0 \le \varphi_i^k \le 2\pi
\end{aligned}
\tag{A.1}
$$

The upper bound for the MINLP problem can be obtained by relaxation. First of all, according to (12), the calculation of c_{ij}^{kq} is very complicated; we can relax it as follows:

$$c_{i,j}^{k,q} = log_2 \left(1 + \frac{p_{i,j}^{k,q}}{N_0} \right); \tag{A.2}$$

Because the terms representing the interference power is removed from the denominator, each individual value of $c_{i,j}^{k,q}$ becomes larger, at least no less than the original definition (12). It is obvious that with the newly defined objective, the upper bound will always be no less than the solution to the original problem.

To relax the third inequality constraint, we can remove the nonlinear term $\gamma \sum_{a=1}^{B} \sum_{b=1,b\neq j}^{N} \sum_{q=1}^{Q} p_{a,j}^{k,q} t_a^{k,q} y_{a,j}^{k,q}$. Then, we get $x_{i,j}^{k,q}(\gamma N_0 + \lambda) - p_{i,j}^{k,q} \leq \lambda$.

For the nonlinear term $t_i^{kj*,q} y_{i,j*}^{kj*,q}$, we can substitute it with a new binary variable $w_i^{kj*,q}$; then, we need to add two more constraints as follows:

$$\begin{aligned} t_i^{kj*,q} + y_{i,j*}^{kj*,q} - w_i^{kj*,q} &\leq 1 \\ t_i^{kj*,q} + y_{i,j*}^{kj*,q} &\geq 2w_i^{kj*,q} \end{aligned} \tag{A.3}$$

With the mentioned three steps, we can reformulate the MINLP problem as a MILP problem, which can be solved by the branch and bound algorithm.

REFERENCES

1. Akyildiz I, Lee W, Vuran M, Mohanty S. Next generation/dynamic spectrum access/cognitive radio wireless networks: a survey. *Computer Networks* September 2006; **50**(13): 2127–2159.
2. Challapali K, Corderiro C, Birru D. IEEE 802.22: The first worldwide wireless standard based on cognitive radios, In *First IEEE International Symposium on New Frontiers in Dynamic Spectrum Access Networks*, Philips Res., Briarcliff Manor, NY, 2005.
3. Guo W, Huang X. Maximizing throughput for overlaid cognitive radio networks, In *Milcom*, Boston, MA, November 2009; 1–7.
4. Guo S, Yang O. Antenna orientation optimization for minimum-energy multicast tree construction in wireless *ad hoc* networks with direction antennas, In *Mobihoc'04*, New York, NY, May 2004.
5. Bandyopadhyay S, Pal M, Saha D, ueda T, Hasuike K, Pal R. Improving system performance of *ad hoc* wireless network with directional antenna, In *IEEE International Conference on Communications (ICC'03)*, Anchorage, Alaska, May 2003; 1146–1150.
6. Hou Y, Shi Y, Sherali H, Wieselthier J. Multicast communications in *ad hoc* networks using directional antennas: a lifetime-centric approach. *Vehicular Technology, IEEE Transactions on* 2007; **56**(3): 1333–1344.
7. Chun P, Wing C, Yue O. Opportunistic routing with directional antennas in wireless mesh networks, In *The 28th Conference on Computer Communications. IEEE*, Orlando FL, April 2009; 2886–2890.
8. Das S, Pucha H, Koutsonikolas D, Hu Y, Peroulis D. DMesh: incorporating practical directional antennas in multichannel wireless mesh networks. *Selected Areas in Communications, IEEE Journal on* 2006; **24**(11): 2028–2039.
9. Mitola J III. Cognitive radio: an integrated agent architecture for software defined radio, *Ph.D. dissertation*, KTH Royal Institute of Technology, 2000.
10. Mitola J, Marguire C Jr. Cognitive radio: making software radios more personal. *Personal Communications, IEEE* August 1999; **6**(4): 13–18.
11. Haykin S. Cognitive radio: brain-empowered wireless communications. *IEEE Journal on Selected Areas in Communications* Febuary 2005; **23**(2): 201–220.
12. Akyildiz I, Lee W, Vuran M, Mohanty S. A survey on spectrum management in cognitive radio networks. *IEEE Communication Magazine* April 2008; **46**(4): 40–48.
13. Thomas R, DaSilva L, MacKenzie A. Cognitive networks, In *First IEEE International Symposium on New Frontiers in Dynamic Spectrum Access Networks*, Baltimore, MD, 2005.
14. Hong Y, Park J. Considerations of multi network in cognitive network, In *10th International Conference on Advanced Communication Technology*, Gangwon-Do, 2008; 341–344.
15. Cao L, Zheng H. Understanding the power of distributed coordination for dynamic spectrum management. *Mobile Network Applications* 2008; **13**(5): 477–497.
16. Chin C, Sim M, Olafssont S. A dynamic channel assignment strategy via power control for *ad hoc* network systems, In *Vehicular technology conference*, Dublin, 2007; 3006–3010.
17. Naveed A, Kanhere S, Jha S. Topology control and channel assignment in multi-radio multi-channel wireless mesh networks, In *IEEE International Conference on Mobile Adhoc and Sensor Systems (MASS)*, Pisa, October 2007; 1–9.
18. Raniwala A, Gopalan K, Chiueh T. Centralized channel assignment and routing algorithms for multichannel wireless mesh networks. *SIGMOBILE Mobile Computer Communications* April 2004; **8**(2): 50–65.
19. Alicherry M, Bhatia R, Li L. Joint channel assignment and routing for throughput optimization in multiradio wireless mesh networks, In *Mobicom*, Cologne, Germany, 2005; 58–72.
20. Ramachandran K, Belding E, Almeroth K, Buddhikot M. Interference-aware channel assignment in multiradio wireless mesh networks, In *Infocom*, Barcelona, Spain, 2006; 1–12.
21. Hu D, Mao S, Reed J. On video multicast in cognitive radio networks, In *IEEE INFOCOM 2009 Proceedings*, Rio de Janeiro, 2009; 2222–2230.
22. Jin J, Xu H, Li B. Multicast scheduling with cooperation and network coding in cognitive radio networks,

In *IEEE INFOCOM 2010 Proceedings*, San Diego, CA, 2010; 1–9.
23. Ren W, Xiao X, Zhao Q. Minimum-energy multicast tree in cognitive radio networks, In *IEEE Asilomar Conference on Signals, Systems, and Computers*, Monterey, CA, 2009; 312–316.
24. Sherali H, Adams W. *A Reformulation-Linearization Technique for Solving Discrete and Continuous Nonconvex Problems*, *chapter 8*. Kluwer Academic Publishers: Norwell, MA, USA, 1999.

AUTHORS' BIOGRAPHIES

Wenxuan Guo received his BS degree in Computer Science and Technology and his MS degree in Information Security from Huazhong University of Science and Technology, Wuhan, China in 2004 and 2007, respectively, and subsequently his PhD degree in Electrical Engineering from Worcester Polytechnic Institute, MA. He currently works at Active Broadband Networks, Inc. His research interest is in resource allocation of wireless networks.

Xinming Huang received his BS and MS degrees in Electrical Engineering from Northwestern Polytechnic University, Xi'an, China in 1994 and 1996, respectively, and his PhD degree in Electrical Engineering from Virginia Tech, Blacksburg, VA in 2001. He is currently an associate professor in the Department of Electrical and Computer Engineering at Worcester Polytechnic Institute, Worcester, MA. He previously worked at the Wireless Advanced Technology Laboratory, Bell Labs of Lucent Technologies. His research interests are in circuits and systems design for embedded computing, including computer architectures, reconfigurable computing, embedded systems, and wireless networks.